Research Article

JOURNAL OF CHEMOMETRICS

Received: 27 September 2010, Revised: 11 November 2010, Accepted: 11 January 2011, Published online in Wiley Online Library: 17 March 2011

(wileyonlinelibrary.com) DOI: 10.1002/cem.1383

Kohonen classification applying '*missing variables*' criterion to evaluate the *p*-boronophenylalanine human-body-concentration decreasing profile of boron neutron capture therapy patients

Jorge Magallanes[a]*, Alejandro García-Reiriz[a], Sara Líberman[a] and Jure Zupan[b]

The irradiation dose in tumor and healthy tissue of a boron neutron capture therapy (BNCT) patient depends on the boron concentration in blood. In most treatments, this concentration is experimentally determined before and after irradiation but not while irradiation is being carried out because it is troublesome to take the blood samples when the patient remains isolated in the irradiation room. A few models are used to predict the boron profile during that period, which until now involves a biexponential decay. For the prediction of decay concentration profiles of the p-boronophenylalanine (BPA) in the human body during BNCT treatment, a Kohonen-based neural network method is suggested. The results of various ($20 \times 20 \times 40$ Kohonen network) models based on different trainings on the data set of 67 concentration sets (profiles) are described and discussed. The prediction ability and robustness of the modeling method were tested by the *leave-one-out procedure*. The results show that the method is very robust and mostly independent of small variations. It can yield predictions, root mean squared prediction error (RMSPE), with a maximum of 3.30 $\mu g\, g^{-1}$ for the present cases. In order to show the abilities and limitations of the method, the best and the few worst results are discussed in detail. It should be emphasized that one of the main advantages of this method is the automatic improvement in the prediction ability and robustness of the model by feeding it with an increasing number of data. Copyright © 2011 John Wiley & Sons, Ltd.

Keywords: artificial neural networks; Kohonen; boron neutron capture therapy (BNCT); tumor irradiation

1. INTRODUCTION

In the boron neutron capture therapy (BNCT) [1], the measurements of the concentration profile of the p-boronophenylalanine (BPA) are carried out *in vivo*. The period in which the measurements should be carried out is variable, for instance 400 min. Unfortunately, the complete profile concentration measurement is not allowed due to the necessity of isolating the patient in the radiation room. Therefore, it is usually stopped between 40 and 60 min after the peak concentration is reached in order to prepare the patient for irradiation. The prediction of the concentration profile of the BPA in blood *after* the last recorded measurement is highly necessary because the radiation dose depends on it. In the present work, the prediction of the concentration profile during the blind period extended up to 4 h is worked out by modeling it with a method based on the Kohonen neural network [2,3] employing the data (concentration profiles) of various lengths recovered from previous treatments reported in the literature [4–9]. The method is described and discussed.

2. DATA

The data set in the study consists originally of 68 concentration profiles recorded at different (not equidistant) time intervals. Profile no. 62 was then discarded (see text below). The concentration profiles consist of 13–33 points all starting with zero time and zero concentration, but ending at a wide variety of time recordings from 250 min up to more than 1400 min. However, most of the profiles have concentrations up to at least 400 min. The distances between the concentration recordings vary considerably among the profiles as well as within each profile; they depend on the readings made at different institutions. An average profile has about five concentrations between the zero point and the maximum one, with the remaining 5–25 points extending over quite different time spans until the final measurement.

* *Correspondence to: J. Magallanes, Comisión Nacional de Energía Atómica, Centro Atómico Constituyentes, Unidad de Actividad Química, Avenida General Paz 1499, San Martín, B1650KNA, Provincia de Buenos Aires, Argentina. E-mail: magallan@cnea.gov.ar*

a *J. Magallanes, A. García-Reiriz, S. Líberman*
Comisión Nacional de Energía Atómica, Centro Atómico Constituyentes, Unidad de Actividad Química, Avenida General Paz 1499, San Martín, B1650KNA, Provincia de Buenos Aires, Argentina

b *J. Zupan*
National Institute of Chemistry, Hajdrihova 19, SLO-1000 Ljubljana, Slovenia

To make the data comparable among themselves, the concentration profiles of the analyzed samples were interpolated to 41 points in 10-min intervals between zero and 400 min. Due to the fact that all profiles have the first point at zero time and zero interval only the remaining 40 points were taken into account for modeling and testing. The profiles that finish before 400 min were extrapolated by the slope of the last available concentration interval recorded. So, the data for making the model consist of the full 67 × 40 data matrix. As input data for the predictions, the same profiles with all points above the maximum plus 60-min interval (six points) cut-offs are used (see flow chart in Figure 1).

Figure 2 shows the data for 67 profiles of the test profiles as they enter the computer as 'unknown profiles' for the predictions. The positions of the maximal values are marked in medium gray and the 6-point difference from the maximal value in darker gray.

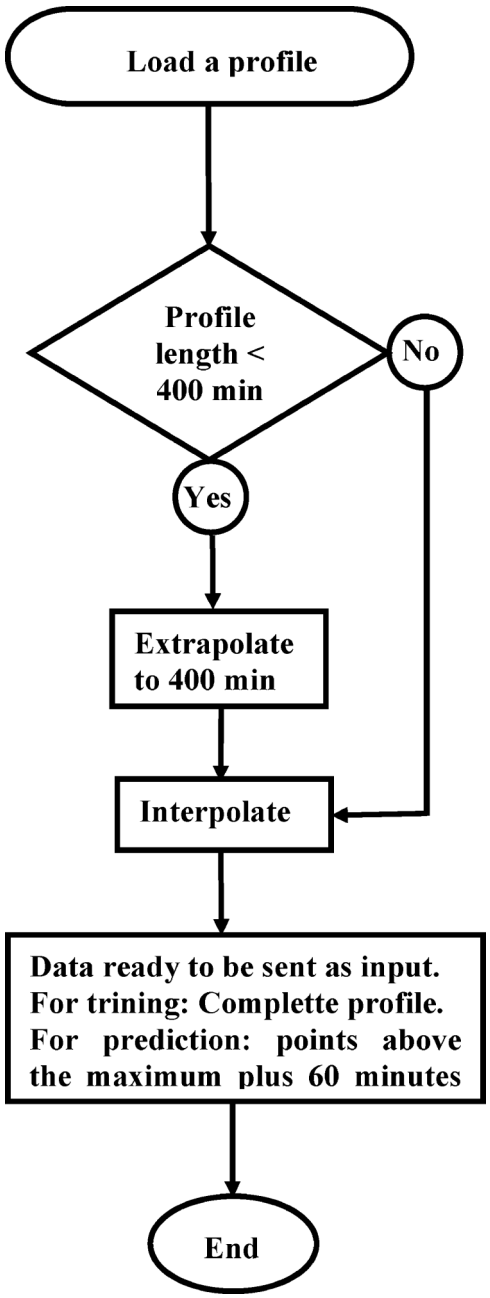

Figure 1. Flow chart of data preprocessing.

The rest of each input profile is filled with the symbol NaN (Not a Number), which are shown by a series of black points in Figure 2, signaling to the computer that the rest of the values are missing.

In order to have a look at the ranges in which the concentration profiles are recorded, the limiting cases are shown in Figure 3. These are the two profiles with the lowest and highest recorded peak concentrations—no. 62 and no. 55, respectively, and the profiles with the shortest and longest time intervals between the start of the drug administration and the time in which the maximal concentration is reached—profile nos 35 and 10, respectively. From now on, profile no. 62 will not be taken into account for statistical purposes because it was obtained by injecting only ½ of the drug concentration; it was initially included to check only the capability of the program for extreme cases.

As it can be seen from Figure 2, not all profiles have the same number of points. Out of 67 profiles, 19 have less than 40 points, with the shortest one extending only up to the 260 min; i.e., it contains 26 concentration points.

3. MODELING METHOD

Kohonen artificial neural network [2,3] was selected as the model because in a special design [10] it can handle inputs of variable lengths. The Kohonen network is an unsupervised method, which means that no target values or target vectors are needed for modeling. Kohonen network is, in principle, a nonlinear two-dimensional clustering of *m*-dimensional objects $\mathbf{X} = (x_1, x_2, \ldots, x_i, \ldots, x_m)$ onto the plane of $N \times N$ neurons. In our case, the Kohonen network consists of 400 neurons distributed in the 20 × 20 plane. Each neuron has 40 weights, which means that the network can be adapted to 40-dimensional objects, or samples, or concentration profiles $\mathbf{X} = (x_1, x_2, \ldots, x_i, \ldots, x_{40})$ (Figure 4).

The additional feature of the used network is that it can handle objects of different lengths, i.e. the profiles having less than 40 concentrations distributed in equidistant 10-min intervals. This feature is achieved by substituting the criterion of the minimal distance *between the neurons* for the determination of the winning neuron in the Kohonen network with the criterion of the minimal distance *between the neurons per one weight* [10].

If the input vector $\mathbf{X} = (x_1, x_2, x_i, \ldots, x_{40})$ has all 40 variable values x_i defined, then all the Euclidean distances between the vector **X** and any neuron $\mathbf{W}_j$ are given by

$$d(\mathbf{X}, \mathbf{W}_j) = \sqrt{\sum_{i=1}^{40} (x_i - w_{ji})^2} \tag{1}$$

On the other hand, with only $m - k$ out of m variables in the object **X** being known, $\mathbf{X} = (x_1, x_2, \ldots x_{m-k}, \text{NaN}, \ldots, \text{NaN})$, the distance between the **X** and any other neuron $\mathbf{W}_j$ can be calculated as a distance per weight, and multiplied by the number of all possible weights:

$$d(\mathbf{X}, \mathbf{W}_j) = m \frac{\sqrt{\sum_{i=1}^{\text{for all } k\, x_i \text{ that are not missed}} (x_i - w_{ji})^2}}{m-k} = \frac{\sqrt{\sum_{i=1}^{\text{for all } k\, x_i \text{ that are not missed}} (x_i - w_{ji})^2}}{1 - \frac{k}{m}} \tag{2}$$

If $k = 0$, Equation (1) yields exactly the same distances in the Kohonen network as the distance *per one weight* in Equation (2).

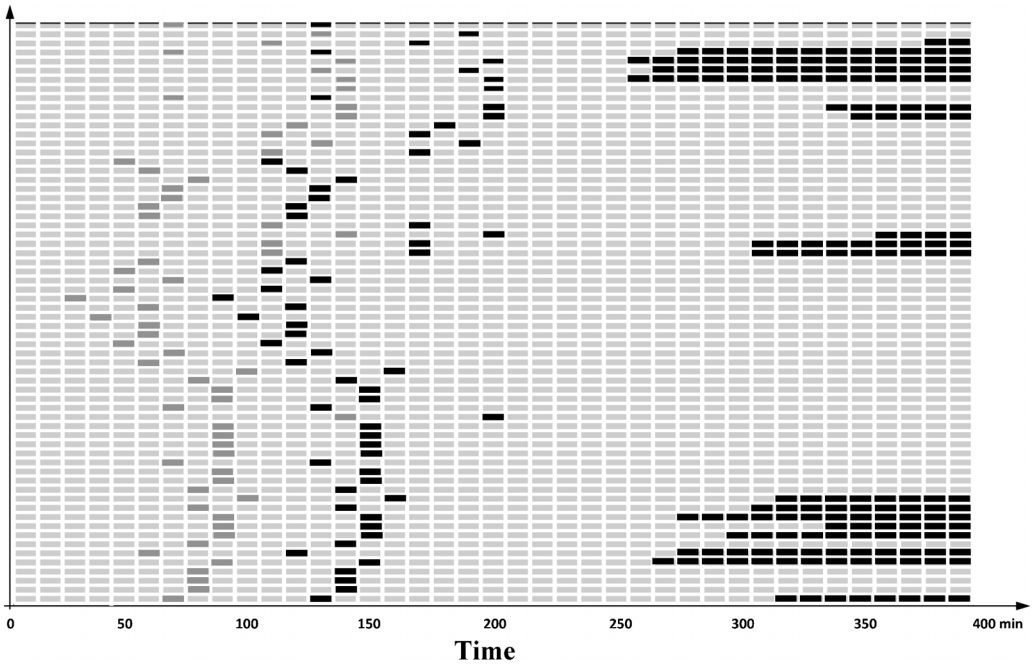

Figure 2. 67 profiles data of the test profiles as they enter in the computer as 'unknown profiles' for the predictions. Light gray points: interpolated data. Medium gray points: peak position. Black points: starting point for predictions. Black point series non-existing data (NaN).

The difference between both distances is the factor (1–*k*/*m*), which means that the search for the smallest distance (for the excited neuron) will yield the same result in both cases even if *k* is not equal to zero. If the input vector **X** has, let us say *three* missing variables, like $\mathbf{X} = (x_1, x_2, \ldots x_{37}, \text{NaN}, \text{NaN}, \text{NaN})$, then the distance calculation between any **X** and all neurons $\mathbf{W}_j$ runs only over 37 values and the winning neuron is determined exactly in the same way with the determination of the smallest distance by Equation (2) as it would be with Equation (1). The sole reason for using Equations (1) or (2) is the determination of the smallest distance between **X** and **W** vectors, without regarding the actual length of **X**.

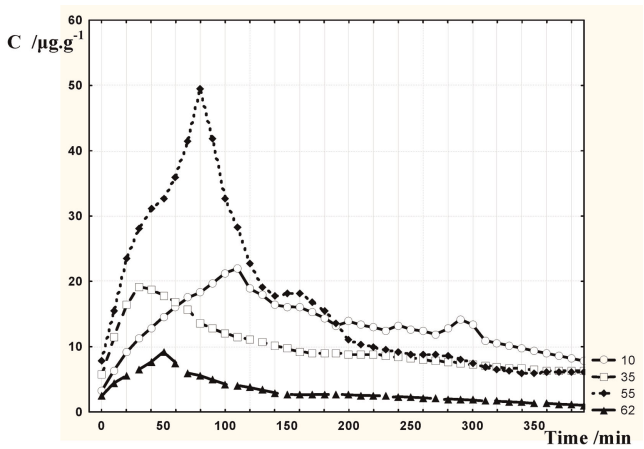

Figure 3. Limit cases in range concentration (profile nos 62 and 55) and shortest and longest time interval between the start of the drug administration and the time in which the maximal concentration is reached (profile nos 35 and 10). Abscissas show time in minutes, and ordinates show boron concentration in $\mu g\, g^{-1}$.

In this way, the Kohonen network weights can be trained with all data including those which have some missing variables. The incomplete data profiles can be entered as the input either to train the Kohonen network or as the unknown input in the case when searching for the most similar neuron in the already trained Kohonen network. In our case, we have used the incomplete data for both events.

As shown in Figure 2, the data collection contains 19 profiles that are not complete. The concentrations are not recorded up to 400 min. For these nineteen profiles, the concentration values stop in the range between 280 and 380 min. One can simply exclude such data out of the study; however, the remaining 49 curves seem to be even less representative than the existing 67, which still form a small group for building a very reliable model. To include such incomplete data, we have tried two approaches for building the models. In the first case, the concentration values beyond the last actually recorded one were obtained by the extrapolation. The extrapolation was made according to the slope between the last two concentration points. In the second approach, the profiles were entered to the training of the Kohonen network as they were obtained up to the last point and the *missing* concentration values up to 400 min added with values of NaN. These values signaled to the program of the Kohonen learning to do the distance calculation according to Equation (2). In Section 4, the prediction results obtained in both ways are compared.

It has to be kept in mind that in the Kohonen neural network *all* weights in *all* neurons in the network are adapted and have specific values depending on the entire neighborhood regardless of whether the neurons were excited during the learning period or not and even if they were excited the values of some specific variables were not defined at all.

The 20×20 Kohonen model has 400 neurons to adapt to 67 concentration profiles $\mathbf{X}_i$, $i = 1, \ldots, 39$ (Figure 4). This was made in 1000 epochs of training, which means that all 67 profiles $\mathbf{X}_i$ were

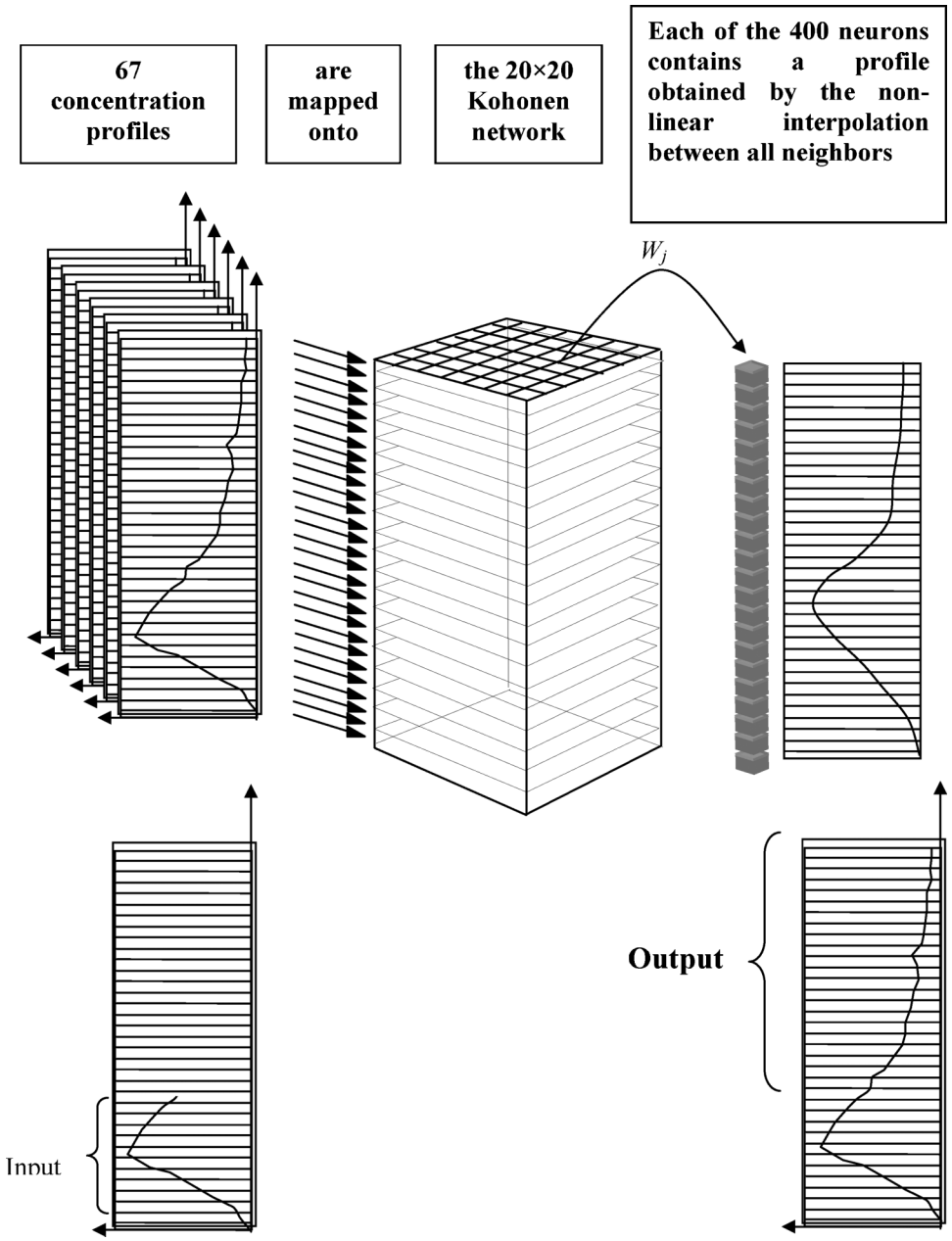

Figure 4. Schematic diagram of the Kohonen network.

sent through the network 1000 times and each profile $\mathbf{X}_i$ was relocated each time according to weight corrections that were constantly adapted to minimize the distance between the inputted profile $\mathbf{X}_i$ and the selected neuron after its input.

4. THE RESULTS

In order to test models, the outputs of which were series of concentrations (boron biodistributions) consisting of several points x_i (each time a different number of them) quantitatively, we have to define a measure of agreement between the sought and the actually predicted result. Taking a complete concentration profile of 40 concentration values as an example of a real case test, then the first, let us say, p points (points up to 60 min after overpassing the maximum) are fed into the computer model as query input, while the remaining $40-p$ points are used for comparison with the predicted data. The quality of the model prediction is the agreement between the actual profile's $40-p$ values (not input into the computer) and the predicted $40-p$ values output by the computer model.

$$d = \frac{\sum_{i=i_{\min}}^{i_{\max}} \left| x_i^{\text{target}} - w_i^{\text{excited}} \right|}{i_{\max} - i_{\min}} = \frac{\sum_{i=i_{\min}}^{40} \left| x_i^{\text{target}} - w_i^{\text{excited}} \right|}{40 - i_{\min}} \quad (3)$$

The summation in Equation (3) runs from the first point of the predicted part of the profile which is 60 min after overpassing

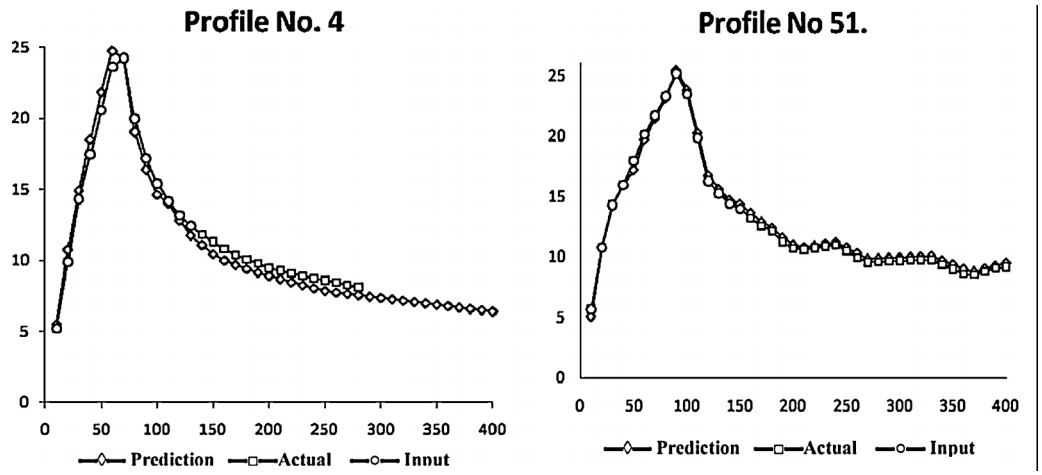

Figure 5. Extreme cases. Two very good cases (see text for details). Abscissas show time in minutes, and ordinates show boron concentration in $\mu g\ g^{-1}$.

the peak to the last point. In the case where the actually tested profile $\mathbf{X}_i^{test}$ has less points than 40, sum (3) stops before, i.e. to $i_{max} < 40$.

The main assumption, of course, is that the profile $\mathbf{X}_i^{test}$ applied in this test was *not used* for the generation of the model and can thus be regarded as an 'unknown' to the computer.

To test the prediction ability of the proposed method, we have cut off all 67 concentration profiles at the time point extending 60 min over the time at which the maximal concentration was reached, i.e. to the maximal point plus six further points. This means that the truncated inputs have between 9 and 20 values, depending on the position of the maximal concentration. The remaining descending concentration profile of 19–30 concentration values has to be predicted if the first part is input to the model. The prediction is based on the winning neuron in the Kohonen network which is excited by the input of the first truncated part of the profile. Because all weights in all 400 neurons in the network are influenced and exposed to the corrections caused by all 67 profiles, each neuron $\mathbf{W}_j$ contains adapted or generated profile which is a result of the completed training procedure in which the complete set of 67 profiles was sent through the Kohonen network several hundred times.

Due to the fact that no two profiles are identical, each profile can easily be identified by few first points' (9–20) concentrations, one value per 10 min. Therefore, it is clear that the ANN prediction of the second part of the profile (19–30) of remaining concentration values is perfect if the profile, of which the first part is used as the input query, was used at the same time for the generation of the ANN model. Hence, this kind of test does not provide the answer about the reliability of the predictions of real cases.

To obtain the actual prediction ability, the *cross-validation leave-one-out* [11,12] procedure was employed. To do this, 67 models were made with 66 actual profiles, leaving out of the modeling procedure one of them each time. Each of these 67 models was tested by only one profile—the one that was left out of the generation of the particular model. Three models with different learning strategies were employed. Due to the fact that all three strategies generate models that yield very similar predictions only the results of the model obtained on the 20×20 network and trained for 300 epochs will be discussed. First, let us have a look at five extreme samples. Two of them, sample nos 4 and 51 (Figure 5), are very good, while the sample numbers 10, 48 and 56 are the worst ones (Figure 6). The first two samples that show very good agreement between the predicted and actual

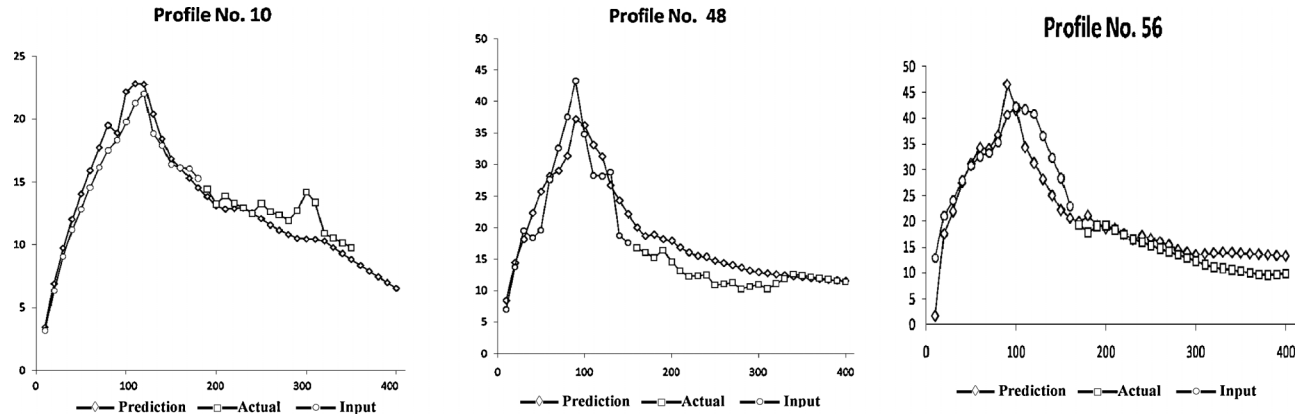

Figure 6. Extreme cases. The three worst cases (see text for details). Abscissas show time in minutes, and ordinates show boron concentration in $\mu g\ g^{-1}$.

Table I. Average concentration's error for each profile at the time of 4 h after the beginning of the treatment for models obtained with different number of epochs and absolute errors at the time of 180 minutes after the beginning

Case no.	Average error 20×20 9999 epochs	Average error 20×20 1000 epochs	Average error 20×20 300 epochs	Concentration at 180 min of the original profile	Error at 180 min 20×20 9999 epochs	Error at 180 min 20×20 1000 epochs	Error at 180 min 20×20 300 epochs
1	3.29	3.34	2.38	14.40	4.71	4.79	3.64
2	0.33	0.48	0.79	13.24	0.25	0.63	0.91
3	3.33	0.46	0.74	13.29	2.86	0.54	0.97
4	0.45	0.49	0.50	10.07	0.63	0.61	0.62
5	1.01	1.20	1.18	19.26	0.98	1.00	1.13
6	0.30	0.90	0.48	13.30	0.05	0.31	0.14
7	1.01	1.03	0.80	18.28	0.98	0.52	0.19
8	0.28	0.28	0.34	13.59	0.12	0.12	0.37
9	1.77	1.77	0.91	12.61	1.76	1.87	0.68
10	2.08	1.74	1.70	15.28	1.71	1.20	1.29
11	0.90	1.40	1.23	14.75	0.49	0.65	0.33
12	0.50	0.93	1.58	16.44	0.04	2.47	0.50
13	0.55	0.55	0.54	12.41	0.31	0.31	0.27
14	2.33	2.27	2.47	16.41	0.53	2.14	1.28
15	1.63	1.77	1.57	13.24	1.50	1.78	1.66
16	2.47	1.15	1.26	16.06	2.40	1.86	1.67
17	0.81	1.60	0.50	10.60	0.06	0.81	0.16
18	2.34	2.16	0.51	10.49	3.91	3.59	0.92
19	3.31	2.03	2.71	9.61	4.60	3.42	3.72
20	1.85	3.90	0.97	14.62	1.89	3.20	1.11
21	0.23	0.36	0.34	9.53	0.04	0.39	0.09
22	1.36	1.78	0.51	10.78	1.08	1.62	0.56
23	0.30	0.30	0.26	12.40	0.25	0.25	0.21
24	2.20	2.81	0.84	13.46	1.81	1.82	0.67
25	0.25	1.00	0.97	16.60	0.20	0.43	0.23
26	0.12	0.10	0.14	15.63	0.12	0.12	0.07
29	1.90	0.68	0.74	13.94	0.27	0.29	0.07
30	0.59	0.69	0.64	10.87	0.27	0.27	0.25
31	1.72	1.71	2.01	13.63	0.61	0.48	0.11
32	0.76	2.47	1.35	10.52	0.92	3.29	0.80
33	1.45	1.80	1.78	11.38	2.36	2.29	2.31
34	0.20	0.21	0.21	9.55	0.26	0.25	0.22
35	2.27	2.74	2.70	9.02	3.25	3.30	3.26
36	1.16	0.72	1.25	9.07	1.09	0.70	1.15
37	0.58	0.69	0.41	11.48	1.05	0.70	0.29
38	0.75	0.89	0.85	9.56	0.96	0.96	0.92
39	0.23	0.45	0.50	9.30	0.50	0.69	0.88
40	2.65	2.65	1.97	14.07	3.56	3.56	3.17
42	1.21	2.45	1.76	15.11	0.64	1.35	0.14
43	1.69	1.85	1.25	13.02	2.35	2.55	2.22
44	2.77	2.47	2.76	22.51	6.49	5.98	6.14
45	0.95	2.05	1.45	11.97	0.55	0.30	0.72
46	2.10	2.23	1.59	13.37	1.33	1.18	0.64
47	1.81	1.02	1.28	16.72	0.61	1.50	2.62
48	2.85	3.41	3.17	15.25	3.94	6.54	5.76
49	3.25	1.78	2.59	13.45	3.15	1.56	2.55
50	0.62	0.84	0.88	16.47	0.01	0.04	0.07
51	0.33	0.35	0.31	12.15	0.26	0.30	0.26
52	2.34	2.36	1.72	11.89	1.56	1.64	1.59
53	5.40	4.70	4.82	21.15	5.13	5.79	5.72
54	1.00	1.23	2.23	10.88	3.76	5.57	4.18

(*Continues*)

Table I. (Continued)

Case no.	Average error 20 × 20 9999 epochs	Average error 20 × 20 1000 epochs	Average error 20 × 20 300 epochs	Concentration at 180 min of the original profile	Error at 180 min 20 × 20 9999 epochs	Error at 180 min 20 × 20 1000 epochs	Error at 180 min 20 × 20 300 epochs
55	1.58	1.29	1.29	13.28	2.53	2.31	2.43
56	2.13	2.13	2.03	17.87	3.28	3.28	3.04
57	1.29	1.79	1.93	17.08	1.57	2.25	2.93
58	2.29	1.46	1.86	16.75	1.24	2.77	1.59
59	0.12	0.10	0.07	15.51	0.12	0.12	0.13
60	4.25	5.61	5.71	12.43	3.76	3.87	3.81
61	2.23	1.96	1.89	4.13	2.06	2.11	2.02
62	2.75	2.76	2.61	1.27	2.85	2.84	2.67
63	1.98	1.86	1.86	2.67	2.35	2.11	2.16
64	4.00	4.42	4.28	16.13	3.25	3.90	3.77
65	0.79	0.57	0.53	12.10	0.91	0.41	0.60
66	1.27	1.49	1.27	13.63	1.45	1.73	1.47
67	1.18	0.97	0.38	16.36	0.61	0.77	0.48
68	1.72	1.35	1.58	15.42	2.09	0.77	1.53
69	2.75	5.04	5.03	17.78	1.98	4.71	4.37
70	1.73	1.62	1.66	15.67	1.22	0.56	0.48
71	1.81	0.31	0.39	16.16	1.38	0.26	0.21

concentration values indicate how good Kohonen model can be if enough data that cover the entire concentration/time space are available. This means that the first two examples show the potential ability of the model. Sample 56 shows that even for a relatively weak agreement between the input query (circular points) and the neuron (rhomboidal points) considerably good predictions can still be obtained.

On the other hand, the two samples, 48 and 10, show different problems that can occur using Kohonen ANN for prediction. In the sample no. 48, one can see extra peaks in the curve which is extremely hard to predict unless the extra peak is an actual reaction for a real pool of patients. Sample no. 10 is an example for a frequent situation when the prediction of the concentration decrease does not match the actual one—it is either too slow or too fast. The problem that in spite of the fact that the input points match the neuron's beginning, a different continuation slope is obtained can be solved only by taking as input as many points as possible for the query. The last sample shows the problem of extrapolation for prediction.

The average root mean squared prediction error (RMSPE) of the 67 CV models is about 3.36 $\mu g\, g^{-1}$. Table I shows the exact average error/concentration point for each profile and the error at the time of 4 h after the beginning of the treatment for models obtained with different number of epochs. Due to the fact that in a 400 (= 20 × 20) neurons Kohonen network which is trained by 67 profiles, at least 333 neurons are empty, i.e. not being excited by a single profile during the training; the excited neuron in the test phase can very probably be one of the empty or not-excited neuron of the network. Such a neuron is result of a dynamic average created by weight adapting process during the training influenced by all incoming profiles. In such a manner, the resulting excited neuron by a truncated input shows a good compromise between all known profiles.

Predictions obtained with this model have been compared against a previous model based on the following bi-exponential algorithm [13].

$$\left.\begin{aligned} C(t) &= \frac{I_0 f}{V_1(\lambda_1-\lambda_2)(t_2-t_1)}\left[\frac{\lambda_1-k_{21}}{\lambda_1}\left(1-e^{\lambda_1 t}\right)+\frac{k_{21}-\lambda_2}{\lambda_2}\left(1-e^{-\lambda_2 t}-1\right)\right], \quad 0 < t \le T_0 \\ C(t) &= \frac{I_0 f}{V_1(\lambda_1-\lambda_2)(t_2-t_1)}\left[\frac{\lambda_1-k_{21}}{\lambda_1}\left(1-e^{\lambda_1 T_0}\right)e^{-\lambda_1(t-T_0)}+\frac{k_{21}-\lambda_2}{\lambda_2}\left(1-e^{-\lambda_2 T_0}\right)e^{-\lambda_2(t-T_0)}\right], \quad t > T_0 \end{aligned}\right\} \tag{4}$$

where $C(t)$ is the BNCT-F concentration at time t, I_0 is the BPA-F infusion constant rate, T_0 is the length of the infusion, V_1 is the volume of body distribution and λ_1, λ_2 and k_{21} are fitting parameters.

This last model has been used until now to fit the complete curve, up and down parts of it, but there were no predictions of the decreasing side using the points from the starting time until those which scarcely overshoot the peak. Being the prediction of the decreasing side of the curve the most important aspect of the modeling in order to work out the radiation's dose of BNCT, we proceeded to recalculate algorithm (4) using the same concept applied for ANN. The error was calculated for each of the original experimental points of the curves located after passing 60 min of the peak's time, using the previous points to calculate the parameters of algorithm (4). The comparisons of the RMSPEs of both methods are shown in Table II.

Table II. Comparisons of the root mean squared prediction errors.

	Kohonen		Biexponential Model	
Case	RMSPE	%RMSPE	RMSPE	%RMSPE
1	1.101	7.79	4.86	36.92
2	0.993	8.16	1.71	14.85
3	0.721	5.58	1.26	10.12
4	0.607	5.70	1.12	11.59
5	0.998	6.11	0.12	0.76
6	0.724	5.98	3.03	26.27
7	0.941	6.14	0	0.01
8	0.333	2.83	2.35	19.99
9	0.735	5.66	0.82	6.32
10	0.776	5.83	0.84	6.44
11	0.970	7.72	2.42	19.24
12	0.317	2.02	8.86	59.37
13	0.023	0.21	3.61	32.51
14	2.713	22.52	6.9	67.31
15	1.680	13.06	1.47	11.41
16	2.489	13.21	1.41	8.22
17	1.060	9.33	3.8	35.7
18	0.609	5.48	2.82	27.06
19	3.021	28.70	4.4	44.43
20	1.850	13.63	1.53	11.6
21	0.334	3.16	1.77	19.57
22	0.326	2.99	2.24	20.58
23	0.897	7.60	1.24	10.61
24	0.476	4.23	2.77	24.65
25	0.518	3.17	1.42	8.69
26	0.382	2.44	2.62	17.77
29	0.419	3.00	1.17	8.96
30	0.059	0.46	0.81	8.36
31	3.000	NA	12.02	118.94
32	1.179	9.64	5.54	45.32
33	1.783	14.15	13.78	109.39
34	0.564	5.58	2.28	23.47
35	0.000	0.00	0.93	9.09
36	3.295	0.00	1.68	18.04
37	0.641	5.24	0.42	3.66
38	0.974	8.12	0.98	9.1
39	0.385	4.15	0.7	7.53
40	1.409	10.21	2.6	20.22
42	0.879	6.08	2.49	18.61
43	1.112	7.64	1.89	12.99
44	2.390	12.20	2.17	11.83
45	1.181	9.97	3.06	25.79
46	1.334	8.46	6.88	46.39
47	2.200	12.55	2.74	16.56
48	3.364	21.68	3.06	21.32
49	0.998	7.75	5.07	42.02
50	0.337	2.08	1.02	6.45
51	0.374	3.24	1.13	9.91
52	0.819	6.84	4.06	34.95
53	0.820	4.31	3.74	19.99
54	3.121	23.78	3.54	28.19
55	2.628	18.37	5.14	35.94
56	1.676	9.05	8.62	46.58
57	2.528	13.45	3.77	20.52
58	1.852	12.00	14.1	106.65
59	0.273	1.76	4.36	29.16
60	1.007	8.26	1.13	10.2
61	0.775	19.08	1.06	27.52
62	1.353	45.09	0.51	19.11
63	1.495	8.68	1.47	9.7
64	0.395	3.08	1.94	15.1
65	1.721	11.80	1.27	8.72
66	0.060	0.34	0.28	1.81
67	2.871	17.50	5.63	42.17
68	0.300	1.70	7.88	43.38
69	0.818	5.14	1.04	6.56
70	0.595	3.67	2.4	14.81

$\%\text{RMSPE} = \frac{\text{RMSPE}}{\overline{C}} \times 100$ $\overline{C}$: Average concentration range.

5. CONCLUSIONS

Until now, standard modeling techniques require, in advance, the knowledge of a mathematical analytical function, the parameters of which are determined on the basis of the best agreement between the experimental and estimated data [4,14,15]. Now, for this model we took advantage of the ANN property of not requiring that knowledge to adapt the relationship between the experimental and estimated data. Then, any experimental deviation of the analytical function shape selected by the previous methods could be successfully traced.

Additionally, in the present work it was shown that the Kohonen neural network model is able to reproduce complex curves from the truncated ones. With the leave-one-out procedure an estimate of the reliability of such model was obtained. Another real advantage of the models of this type is that it could be constantly improved by adding new data to the training matrix.

Acknowledgements

The authors thank Dr Sara J. Gonzalez for her kind provision of data. Part of the work was financed through the Argentina-Slovenia bilateral project SLO/08/12 and Agency for Research of Republic of Slovenia through the Programme P1-0017.

REFERENCES

1. Barth RF, Coderre JA, Vicente MGH, Blue TE. Boron neutron capture therapy of cancer: current status and future prospects. *Clin. Cancer Res.* 2005; **11**: 3987–4002.
2. Zupan J, Gasteiger J. *Neural Networks in Chemistry and Drug Design*. Wyley-VCH: Verlag, Germany, 1999.
3. Kohonen T. *Self-Organizing Maps*. Springer-Verlag, Springer: Berlin, Heidelberg, Germany, 1995.

4. Ryynänen P, Kangasmäki A, Hiismäki P, Coderre J, Diaz AZ, Kallio M, Laakso J, Kulvik M, Savolaineen S. Non-linear model for the kinetics of ^{10}B in blood after BPA-fructose complex infusion. *Phy. Med. Biol.* 2002; **47**: 737–745.
5. Kiger WS, III Palmer MR, Zamenhof RG, Busse PM. Boron uptaken by erythrocytes following boronophenylalanine-fructose infusion in humans. *Proceedings Ninth International Symposium on Neutron Capture for Cancer*, Osaka, Japan, 2000. 23–24.
6. Capala J, Stenstam BH, Sköld K, Rosenschöld PM, Giusti V, Persson C, Wallin E, Brun A, Franzen L, Carlsson J, Salford L, Celeberg C, Persson B, Pellettieri L, Henriksson R. Boron neutron capture therapy for glioblastoma multiforme: clinical studies in Sweden. *J. Neuro Oncol.* 2003; **62**: 135–144.
7. Kiger WS, III, Palmer MR, Riley KJ, Zamenhof RG, Busse PM. A Pharmacokinetic model for the concentration of ^{10}B in blood after boronophenylalanine-fructose administration in human. *Radiat. Res.* 2001; **155**: 611–618.
8. Coderre JA, Elowitz EH, Chadha M, Bergland R, Cepala J, Joel DD, Liu HB, Slatkin DN, Chanana DA. Boron neutron capture therapy for glioblastoma multiforme uing *p*-boronophenylalanine and epithermal neutrons: Trial desing and early clinical result. *J. Neuro Oncol.* 1997; **33**: 141–152.
9. Riley KJ. Improved ^{10}B Quantification via PSNAA and ICP-AES. *Master Sci. Thesis*. Nuclear Engeneering, MIT, 1997.
10. Zupan J, Novič M, Ruisánchez I. Kohonen and counterpropagation artificial neural networks in analytical chemistry. *Chemom. Intell. Lab. Syst.* 1997; **38**: 1–2.
11. Haaland DM, Thomas EV. Partial least-squares methods for spectral analyses. 1. Relation to other quantitative calibration methods and the extraction of qualitative information. *Anal. Chem.* 1988; **60**: 1193–1202.
12. Brereton RG. *Chemometrics. Data Analysis for the Laboratory and Chemical Plant*. Wiley: Chichester, UK, 2003.
13. Kiger WS, III Palmer MR, Riley KJ, Zamenhof RG, Busse PM. Pharmacokinetic modeling for boronophenylalanine-fructose mediated neutron capture therapy: ^{10}B concentrarion predictions and dosimetric consequences. *J. Neuro Oncol.* 2003; **62**: 171–186.
14. Ryynänen P, Kortesniemi M, Coderre JA, Diaz AZ, Hiimäki P, Savolainen SE. Models for estimation of the ^{10}B concentration after BPA-fructose complex infusion patients during epithermal neutron irradiation in BNCT. *Int. J. Radiat. Oncol. Biol. Phys.* 2000; **48**: 1145–1154.
15. Kortesniemi M, Seppälä T, Auterinen I, Savolainen S. Enhanced blood boron concentration estimation for BPA-F mediated BNCT. *Appl. Radiat. Isot.* 2004; **61**: 823–827.

